

1 Carbohydrate Polymers

2 Volume 194, 15 August 2018, Pages 51-60

3 <https://doi.org/10.1016/j.carbpol.2018.04.025>

4 <https://www.sciencedirect.com/science/article/pii/S014486171830403X>

5
6 Cellulose nanocrystal/amino-aldehyde biocomposite films

7
8 *Sebestyén Nagy¹, Emília Csiszár^{1,*}, Dávid Kun^{1,2} and Béla Koczka³*

9 ¹Laboratory of Plastics and Rubber Technology, Department of Physical Chemistry and
10 Materials Science, Budapest University of Technology and Economics, H-1111 Budapest,
11 Műegyetem rkp. 3., Hungary

12 ²Institute of Materials and Environmental Chemistry, Research Centre for Natural Sciences,
13 Hungarian Academy of Sciences, H-1117 Budapest, Magyar tudósok körútja 2., Hungary

14 ³Department of Inorganic and Analytical Chemistry, Budapest University of Technology and
15 Economics, H-1111 Budapest, Szt. Gellért tér 4., Hungary

16
17
18
19
20
21
22

*Corresponding author.

Tel.: +36 1 463 1423; fax: +36 1 463 3474. Email address: ecsiszar@mail.bme.hu (E. Csiszár).

23 Abstract

24 From the suspensions of cellulose nanocrystals (CNCs) derived from cotton and flax
25 by acidic hydrolysis, transparent and smooth films were produced with different plasticizers
26 and an amino-aldehyde based cross-linking agent in a wide composition range by a
27 simultaneous casting and wet cross-linking process. The effect of cross-linker concentration
28 on the optical and tensile properties and on the morphology of CNC films was investigated by
29 various measurements. The interaction of films with liquid water and water vapour was also
30 characterized by water sorption and water contact angle as well as performing a sinking test.
31 Cross-linking improved the transparency, reduced the porosity and surface free energy, and
32 prevented the delamination of CNC films in water at a concentration of 10 % or higher. The
33 surface of CNC films is basic in character and has an electron donor property. The
34 CNC/amino-aldehyde films had a high tensile strength (45 MPa) and modulus (11 GPa).

35 1. Introduction

36 Nanocrystalline cellulose, which can be extracted from cellulose-based materials by an
37 acidic hydrolysis, consists of rod-like nano-sized crystals of cellulose and possesses several
38 attractive properties, such as versatile fibre morphology, easy surface modification, large
39 surface area and high aspect ratio (Klemm et al., 2011; Tang, Sisler, Grishkewich, & Tam,
40 2017). Cellulose nanocrystals (CNCs) have been used for various applications, such as
41 antimicrobial/antiviral systems, tissue engineering, drug/gene delivery, biosensors, adsorbents
42 in wastewater treatment, super-capacitors, conductive films, electronic sensors, Pickering
43 emulsifier, drilling fluid, antioxidant or food additive/packaging. In recent years, there has
44 been an increasing interest in the production of transparent thin films of CNCs with special
45 properties and the number of research papers published in this field has been growing
46 exponentially (Lagerwall et al., 2014; Majoinen, Kontturi, Ikkala, & Gray, 2012; Sun et al.,
47 2018; Tang et al., 2017).

48 CNC films are highly hydrophilic and this property can limit their applications in certain
49 areas. Water sorption of CNC films was found to be similar to that of MFC films (around 25-
50 30 % mass gain), and the water contact angle was around 45° (Belbekhouche et al., 2011).
51 The thickness of CNC ultrathin films changed proportional to the changes in relative
52 humidity. At the point of hydration, each individual CNC in the film became enveloped by a 1
53 nm thick layer of adsorbed water vapour (Niinivaara, Faustini, Tammelin, & Kontturi, 2015).

54 To improve the properties of films and to modify their interaction with water, the
55 cellulose in CNC films is usually cross-linked during or after casting. In chemical cross-
56 linking, polymer chains are interconnected by permanent covalent bonds, which results in a
57 brittle product (Peng, Zhai, She, & Gao, 2015; Yang, Zhao, Xu, & Sun, 2013). Chemical
58 cross-linking of cellulose is a well-known reaction in the field of textile finishing and can be

59 carried out in a heterogeneous system with various aldehydes. However, only formaldehyde,
60 glutaraldehyde and glyoxal cross-link successfully the cellulose, resulting in wrinkle recovery
61 cellulosic textiles (Frick & Harper, 1982; Kim & Csiszár, 2005). Commonly used cross-
62 linking agents are amino-aldehyde compounds (such as urea-formaldehyde and melamine
63 formaldehyde) which are widely applied to improve the wearing and easy-care properties of
64 cellulosic textiles.

65 The cross-linking can be carried out in fully swollen or partially swollen fibres (both are
66 called as wet cross-linking), or in dry state (so-called dry cross-linking). Depending on the
67 accessibility and reactivity of the different cellulose areas, conversion of cellulosic fibres can
68 progress to various degrees. Three different situations are possible in the reactions: (1)
69 formation of one covalent bond between the cross-linker and a cellulose chain; (2) formation
70 of at least two covalent bonds between the cross-linker and a cellulose chain (intra-chain
71 linkage); (3) formation of at least two covalent bonds between the cross-linker and two
72 cellulose chains (cross-linking). All of these reactions affect the properties of cellulosic
73 substrates in a greater or lesser degree. Cross-linking has the most significant and distinctive
74 effects (Krässig, 1993; Rouette, 2002). In optimal conditions, the amino-aldehyde based pre-
75 polymers mixed with cellulose lead to composite formation (Devallencourt, Saiter, &
76 Capitaine, 2000).

77 Aldehyde-aided cross-linking was also used in the preparation of nanocellulose films
78 with advanced properties. Nanocomposite films of microfibrillated cellulose (MFC) and
79 melamine formaldehyde (MF) were semi-transparent, stiff and brittle, and their density
80 increased with increasing MF content (Henriksson & Berglund, 2007). Moisture sorption of
81 the MFC/MF films was lower than that of the neat MFC films, due to the interaction between
82 the resin and the hydroxyl groups of the cellulose surface, which left fewer hydroxyl groups
83 accessible for water molecules. The maximum of Young-modulus, 19.3 GPa was measured

84 for the MFC/MF nanocomposite films. Besides cross-linking, only the introduction of a cross-
85 linker to nanocellulose can also enhance the water repellence of nanocellulose films by filling
86 the pores in it and reducing polarity. Improvements in the mechanical properties of films were
87 also achieved by increasing the water repellence, since water itself acts as a plasticizer in
88 nanocellulose films (Henriksson & Berglund, 2007).

89 Extensive work has been done on using cross-linking agents different from aldehydes.
90 Thermo-responsive and water-responsive shape-memory polymer nanocomposites were
91 developed by chemically cross-linking cellulose nanocrystals with polycaprolactone (PCL)
92 and polyethylene glycol (Liu, Li, Yang, Zheng, & Zhou, 2015). Since PCL is hydrophobic, it
93 may be used to develop water repellent CNC composites. As the ratio of nanocellulose to
94 PCL decreased, the water repellence of PCL-nanocellulose nanocomposites increased (Si,
95 Cui, Wang, Liu, & Liu, 2016). Poly(acrylic acid) was used as a cross-linking agent in a
96 poly(vinyl alcohol)/CNC nanocomposite. The formation of ester linkages between poly(vinyl
97 alcohol) and CNC resulted in a highly networked structure and improved mechanical
98 properties (Pakzad, Simonsen, & Yassar, 2012). Cross-linking of nanocellulose with citric
99 acid has also been studied (Quellmalz & Mihranyan, 2015). For other biopolymers such as
100 polyhydroxyalkanoates, cross-linking was also beneficial and a significant improvement in
101 the mechanical properties and water resistance of composites was achieved (Raza, Riaz, &
102 Banat, 2017).

103 In spite of the fact that amino-aldehyde based compounds are the most frequently used
104 cross-linking agents of cellulose and they are widely applied in the field of finishing of
105 cellulosic textiles, very little is known about their use in cross-linking of nanocrystalline
106 cellulose. Thus the goal of our study was to prepare cellulose nanocrystal/amino-aldehyde
107 (CNC/AA) nanocomposite films, to demonstrate the effect of wet cross-linking of cellulose
108 on the structure and properties of nanocrystalline cellulose-based thin films, and to evaluate

109 the interaction of films with water as a function of cross-linking. Cellulose nanocrystals were
110 extracted from bleached cotton and flax fibres by sulphuric acid hydrolysis. Two plasticizers
111 (sorbitol and glycerol) were used for casting a series of films with an amino-aldehyde (AA)
112 based cross-linking agent applied in a wide range of concentrations. The results proved that
113 the properties of CNC films can be enhanced and tuned by the amino-aldehyde based cross-
114 linking of cellulose.

115 2. Experimental

116 2.1 Preparation of cellulose nanocrystals

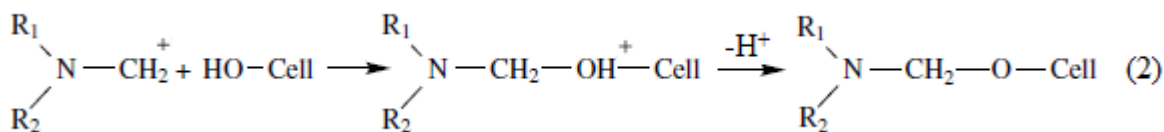
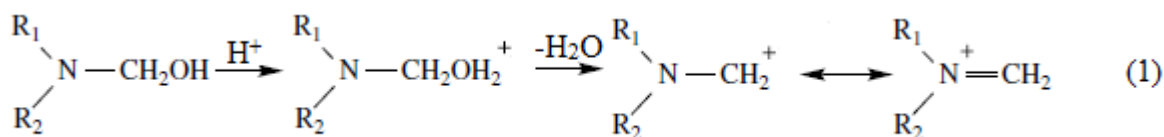
117 CNCs were prepared from bleached cotton and flax plain-weave fabrics (110 g/m² and
118 165 g/m², respectively) provided by Pannon-Flax Linen Weaving Co. (Hungary) and used
119 without any further wet treatment. The nanocrystals were denoted as cotton-CNC and flax-
120 CNC, depending on the source of cellulose. The fabrics were ground using a ball mill (Mixer
121 Mill MM400, Retsch GmbH, Germany), then 10.0 g of the fine powders were hydrolyzed
122 with 64 wt % sulphuric acid (acid to fibre ratio: 8.75 ml/g) at 45 °C for 25 min (Hamad & Hu,
123 2010). Subsequent to the post-treatments (washing, centrifugation and dialysis), the total
124 volume of the stock suspensions was subjected to ultrasonication for 10 min using an
125 ultrasonic horn type reactor (Vibra-Cell VCX500, Sonics & Materials, Inc. CT, USA) at 60 %
126 amplitude with a driving frequency of 20 kHz (Csiszar, Kalic, Kobol, & Ferreira, 2016). The
127 dry solid content of the suspension was determined by drying (at 80 °C) and weighing 2 ml of
128 the suspension. Yield of CNC calculated as a percentage of the initial weight of the bleached
129 fibres was in the range of 41-43 %. The final aqueous suspensions contained 2-3 weight % of
130 CNCs.

131 *2.2 Preparation of films from the CNC suspensions*

132 Rectangular films were cast from the aqueous suspension of CNCs on the surface of a
133 polypropylene plastic sheet, and their water content was allowed to evaporate at room
134 temperature for about 2 days. In order to overcome the brittle nature of the CNC films, two
135 different plasticizers, namely sorbitol and glycerol were added in 20 % concentration (Csiszár
136 & Nagy, 2017). These polyhydroxy compounds were already successfully applied as
137 plasticizers for thermoplastic starch films (Mathew & Dufresne, 2002).

138 For the cross-linking of cellulose nanocrystals, an amino-aldehyde based, water
139 soluble cross-linking agent (dimethylol-dihydroxy-ethylene-urea) with an acidic catalyst
140 (trade names: Reaknitt B-FV and Reaknitt Catalyst FV, respectively, received from Bezema
141 AG, Switzerland), recommended for wet cross-linking of cellulosic textiles, were added in
142 different percentages (0, 2.5, 5, 10, 20, 30, 50 % and 0, 0.75, 1.5, 3.3, 6.6, 10, 16.7 %,
143 respectively) on a dry CNC basis to the CNC suspensions before casting. Both the cross-
144 linking agent and the catalyst were commercialized in water as solvent medium. The cross-
145 linking reaction of cellulose took place in the presence of the applied catalyst for about 2 days
146 at room temperature. The thickness of films was in the range of 31-44 μm and slightly
147 increased with increasing the concentration of the cross-linking agent.

148 The chemical reaction between the amino-aldehyde based cross-linking agents and the
149 hydroxyl groups of cellulose usually takes place with addition of acidic catalyst, which acts as
150 a reaction trigger and accelerator. Acidic catalyst breaks the carbon-oxygen linkage in the N-
151 methylol group of the AA-based cross-linker with discharging of water (equation 1) and then
152 catalyses the reaction with a hydroxyl group of cellulose (equation 2) (Rouette, 2002).



153

154

155

156

157

158

159

160

161

162

Conditioning and determining the physical and mechanical properties of the detached

films were carried out in a test laboratory where the temperature and humidity were controlled

to 23 °C and 55 %, respectively. Since cotton-CNC and flax-CNC films containing either

sorbitol or glycerol plasticizers and an amino-aldehyde based cross-linking agent were

produced in a relatively wide composition range, films with selected compositions were only

investigated in some of the experiments. Furthermore, the films prepared with 50 % cross-

linking agent content were characterized exclusively by tensile properties in order to find out

whether the tensile strength was a maximum or not at a cross-linking agent concentration of

30 %.

163

2.3 Characterization of CNC films

164

From the suspensions, transparent and smooth thin films were cast. Transparency was

165

characterized by the transmittance values measured at 600 nm using a Unicam UV 500 (USA)

166

spectrophotometer. For measuring the haze, films were tested by a Color Quest XE

167

(HunterLab, Reston, USA) spectrophotometer. Haze specifies the percentage of transmitted

168

light that while passing through the specimen, deviates from the incident beam by more than

169

2.5 ° (Wang, Kamal, & Rey, 2001).

170

Morphology of the films was characterized by scanning electron microscopy (SEM)

171

using a JEOL JSM 6380 LA equipment. SEM micrographs were taken of the fracture surface

172

of films which were frozen in liquid nitrogen and subsequently broken. For determining the

173

density of films, the weight of 13 specimens from each of the films in different series as well

174 as their area and thickness were measured. Then, for the determination of film porosity the
175 theoretical pore-free density of films was calculated from the density of film components
176 weighted by their mass fraction. Density values of 1.57, 1.49, 1.26 and 1.4 g/cm³ were used
177 for the CNCs, sorbitol, glycerol and the amino-aldehyde based cross-linker, respectively. In
178 the calculation, the density of air was neglected (Henriksson & Berglund, 2007). The
179 following formula was used for the calculation of porosity:

$$180 \text{ Porosity (\%)} = (\text{theoretical density} - \text{measured density}) / (\text{theoretical density}) \times 100 \quad (3)$$

181 Density and porosity data were used for statistical analysis, where the univariate analysis of
182 variance (ANOVA) was applied. Parameters of the fitted trend-lines were calculated by
183 regression analysis. Details of the statistical tests are included in the Supporting Information.

184 Contact angles were measured at 23 °C and 55 % relative humidity using a Rame-Hart
185 contact angle goniometer (USA) with a camera and a drop image standard software of DT-
186 Acquire. Liquid drops of 20 µl were deposited on each film and the image of drops was
187 captured immediately by the camera. The values reported are the average of contact angles of
188 at least 5 drops for each sample. To calculate the surface energy of the CNC films, contact
189 angle measurement was carried out with two liquid probes: distilled water and diiodomethane
190 (Sigma Aldrich, 99%); and from the equilibrium contact angle data the surface free energy
191 was calculated by the Owens-Wendt formula (Owens & Wendt, 1969):

$$192 \gamma_{LV}(\cos\theta + 1) = 2(\gamma_{LV}^d \gamma_{SV}^d)^{1/2} + 2(\gamma_{LV}^p \gamma_{SV}^p)^{1/2} \quad (4)$$

193 where γ_{LV} , γ_{LV}^d and γ_{LV}^p are the surface tension of the liquid and that of its dispersion and polar
194 components, respectively, used in the measurements. The values of γ_{LV} , γ_{LV}^d and γ_{LV}^p used for
195 the calculations are 72.8, 21.8 and 51.0 mJ/m² for distilled water, and 51.0, 51.0 and 0 mJ/m²
196 for diiodomethane. γ_{SV}^d and γ_{SV}^p are the dispersion and polar components of the surface free

197 energy of films, respectively. The total surface free energy of the films was calculated by the
198 following equation:

$$199 \quad \gamma_S^{total} = \gamma_{SV}^d + \gamma_{SV}^p \quad (5)$$

200 Moisture regain (based on the dry weight of films) at 55 % relative humidity was
201 determined using a Denver Instrument IR-35 (USA) moisture analyzer. Two sinking tests
202 were developed for characterising the swelling behaviour of CNC films in liquid water. (1) In
203 the dynamic sinking test, a film sample (1×1 cm) was laid gently onto the surface of distilled
204 water (50 ml) under orbital shaking at 100 rpm (Boeco OS 20, Germany) at room
205 temperature, and the elapsed time for the complete immersion of the film (if any) was
206 recorded. (2) In the static sinking test the measurement introduced above was carried out but
207 without shaking and for 24 hours. The extent of swelling was characterized by measuring the
208 water uptake of films. After floating or immersion for 24 hours, the excess water was
209 removed from the surface of samples and the mass was measured. Water uptake as a
210 percentage of dry weight (weight of water/initial dry weight of the film) was calculated.
211 Furthermore, each of the films from the static sinking test was dried and the percentage
212 weight loss of the initial dry weight of films was also calculated in order to characterize the
213 delamination of nanocrystals and/or dissolution of components in the nanocomposite films (if
214 any) occurring during the 24-hour test.

215 The crystalline structure of cellulose in films plasticized with both plasticizers and prepared
216 with or without 10 or 30 % cross-linking agent content was characterized by X-ray diffraction
217 (XRD) using a Philips PW 1710/PW 1820 diffractometer at $2\theta=4-40^\circ$. To define the
218 crystallinity index (CrI), the following equation was used:

$$219 \quad \text{CrI (\%)} = (1 - I_{AM}/I_{200}) \times 100 \quad (6)$$

220 where I_{AM} denotes the intensity of diffraction at $2\theta=18^\circ$, and I_{200} represents the maximum
221 intensity of the 200 lattice diffractions at $2\theta=22.7^\circ$ (Segal, Creely, Martin, & Conrad, 1959).

222 Mechanical properties were examined using an Instron 5566 tensile tester (USA)
223 equipped with a 500 N load cell. At least ten specimens with the size of 7×50 mm were cut
224 from each of the films in different series. They were tested at 10 mm/min cross-head speed
225 and with 20 mm span length. Linear trend lines were fitted to the initial steep sections of
226 typical stress strain curves of films, in order to determine the Young's modulus of films (He et
227 al., 2016).

228 3. Results

229 *3.1 Transparency and haziness*

230 Smooth and transparent films with a thickness of c.a. 40 µm were cast from the aqueous
231 suspensions of cellulose nanocrystals, and then the water content was evaporated. Besides
232 plasticizers (i.e. glycerol and sorbitol), different amount of an amino-aldehyde cross-linker
233 was added to the suspension in order to investigate the effect of wet cross-linking on the
234 structure and properties of the cotton-CNC and flax-CNC films. UV-vis spectra proved that
235 none of the films has significant absorbance in the wavelength range of visible light (Table 1),
236 and they are transparent and colourless. However, there are some differences in the
237 transparency of films. The flax-CNC films and the films plasticized with glycerol are less
238 transparent than the cotton-CNC and the sorbitol plasticized films, respectively. Also, when
239 adding cross-linking agent, the transmittance values at 600 nm are slightly increasing.

240

241

242

243

244

245 **Table 1**

246 Transmittance and crystallinity index of cotton-CNC and flax-CNC films plasticized with
 247 sorbitol or glycerol and prepared with different amount of amino-aldehyde based cross-
 248 linking agent.

Characte- ristics	Source of cellulose	Type of plasticizer	Concentration of cross-linking agent (%)					
			0	2.5	5	10	20	30
Transmittance (%) ^a	Cotton	Sorbitol	73	80	82	83	83	83
		Glycerol	74	79	82	81	78	80
	Flax	Sorbitol	72	75	77	79	79	80
		Glycerol	70	72	73	78	75	74
Crystallinity index (%) ^{b,c}	Cotton	Sorbitol	93.6	- ^d	-	93.3	-	91.7
		Glycerol	93.3	-	-	88.0	-	87.3
	Flax	Sorbitol	89.7	-	-	85.4	-	85.2
		Glycerol	88.4	-	-	83.6	-	83.5

249 ^a At 600 nm

250 ^b Determined by XRD.

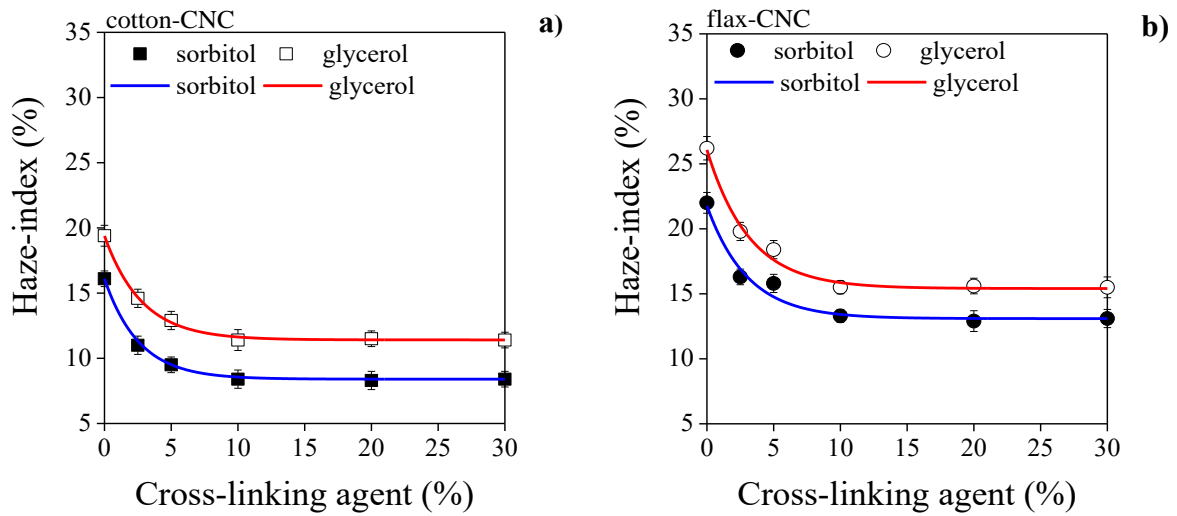
251 ^c Crystallinity of the cellulose sources, namely the ground bleached cotton and flax: 75.9 % and
 252 64.8 %, respectively (Csiszár & Nagy, 2017).

253 ^d - Not determined.

254 Haze-index data correlate well with the transmittance values and reveal in general that
 255 cotton-CNC films are less hazy (Fig. 1a) than the flax-CNC films (Fig. 1b), and the haze-
 256 indices are in the range of 8-20 % and 14-27 %, respectively. Moreover, films plasticized with
 257 sorbitol show lower haze-index (8-23 %) than those plasticized with glycerol (12-27 %).

258 Thus, the flax-CNC films plasticized by glycerol show the highest values of haze-index.

259 However, they are still transparent.



260

261 **Fig. 1.** Haze-index of cotton-CNC (a) and flax-CNC (b) films, plasticized with sorbitol or

262 glycerol, as a function of amino-aldehyde based cross-linker concentration.

263 Concerning the effect of cross-linking agent on the haziness of films, it is obvious that

264 when the AA cross-linking agent concentration increases, the haze-index first decreases and

265 then levels off at 10 % cross-linking agent content (Fig. 1). The tendency and shape of curves

266 are similar for each series of films, however, the minimum values are different for each. The

267 lowest haze-index is around 8 and 12 % for cotton-CNC films and 13 and 16 % for flax-CNC

268 films plasticized with sorbitol and glycerol, respectively. Furthermore, the addition of cross-

269 linking agent leads to formation of films with very smooth surface compared to the structure

270 of other surfaces. This can also influence haziness, since a rougher surface deflects more light

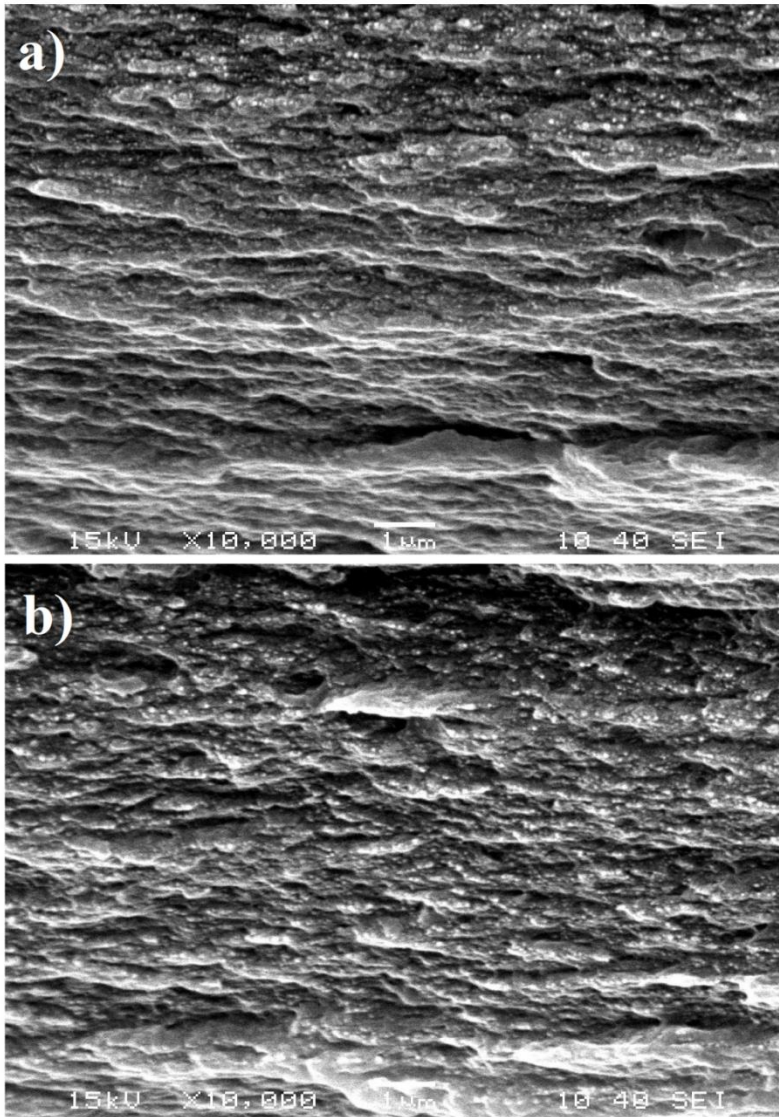
271 than a smoother one (Roy Choudhury, 2014).

272 3.2 Morphology

273 Scanning electron micrographs were taken to characterize the morphology of CNC

274 films by examining the surfaces fractured at the boiling point of liquid nitrogen. The effects of

275 cellulose source (cotton, flax), type of plasticizer (sorbitol, glycerol) and the amount of
276 amino-aldehyde cross-linking agent were examined. The scanning electron micrographs of
277 plasticized films from different sources confirmed our earlier observations that neither the
278 source of cellulose nor the type of plasticizer affect significantly the inner morphology and
279 structure of CNC films (Csiszár & Nagy, 2017). Adding 30 % cross-linking agent to the CNC
280 suspension before film casting, however, leads to a slightly rougher fractured surface, as it is
281 demonstrated for flax-CNC films in Fig. 2. Consequently, films with cross-linking agent have
282 a slightly tougher structure, which presumably occurs because of cross-linked nanocrystals.
283 Researchers examined SEM images of CNC dry film cross sections and found that cellulose
284 nanocrystals exhibit a self-assembled, closely packed layer-by-layer arrangement in dry films
285 (Abraham et al., 2016; Csiszár & Nagy, 2017), which can be seen also in the SEM images of
286 Fig. 2. This phenomenon was explained by the liquid crystalline properties and anti-parallel
287 crystalline arrangement of cellulose I β structure, which was proven by ^{13}C -NMR
288 spectroscopy (Larsson, Hult, Wickholm, Pettersson, & Iversen, 1999).

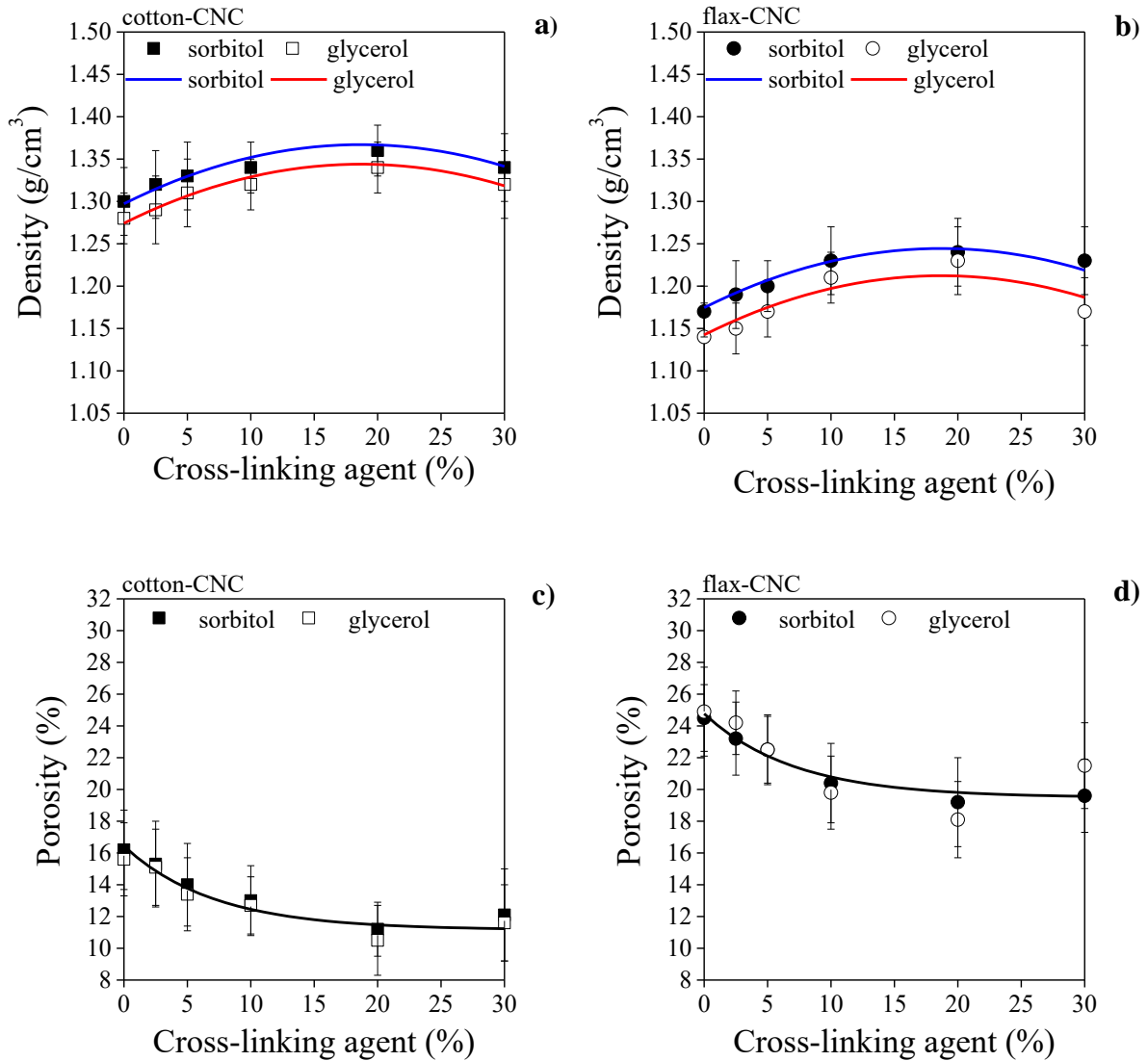


289

290 **Fig. 2.** Scanning electron photomicrographs of the fractured surface of flax-CNC films: (a)
291 plasticized with 20 % glycerol; (b) plasticized with 20 % glycerol and cross-linked with 30 %
292 amino-aldehyde based cross-linking agent.

293 Changes in morphology of CNC-nanocomposite films were further characterized by
294 measuring density and porosity values. Density data of the sorbitol plasticized cotton-CNC
295 films (Fig. 3a) reveal that by increasing the concentration of cross-linking agent to 20 %,
296 density grows from 1.30 ± 0.04 to 1.36 ± 0.03 g/cm³, as AA fills the pores between
297 nanocrystals. By further increasing the cross-linking agent content from 20 to 30 %, the
298 density values slightly decrease after passing the maximum reached at about 20 %. This is

299 accounted for the lower density of cross-linking agent (1.4 g/cm^3) compared to that of
 300 cellulose nanocrystals (1.57 g/cm^3). Films plasticized by glycerol and made from flax-CNC
 301 follow similar trends, but differences are observed mainly between the values of cotton-CNC
 302 and flax CNC films (Figs. 3a and b). Density of MFC films (around 1.34 g/cm^3) (Henriksson
 303 & Berglund, 2007) was found to be similar to that of CNC films.



304

305

306 **Fig. 3.** Density (a, b) and porosity (c, d) of CNC films from cotton (a, c) and flax (b, c),
 307 plasticized with sorbitol or glycerol, as a function of amino-aldehyde based cross-linker
 308 concentration.

309 Sorbitol plasticized films show higher density than glycerol plasticized ones.
310 Moreover, cotton-CNC films are denser than flax-CNC films (Figs. 3a and b). Results fit with
311 an earlier study on plasticized CNC films (Csiszár & Nagy, 2017). It should be mentioned that
312 the standard deviation of each sample is notable. However, statistical analysis showed that
313 cellulose source, plasticizer type and also the amount of cross-linking agent significantly
314 affects the density values of films ($p < 0.05$). An empirically selected quadratic polynomial
315 correlation was fitted in the graph of density versus the amount of cross-linking agent, and
316 maximum density is reached at approximately 20 % cross-linking agent content. Analysis of
317 variance indicated that there is no significant difference between the shapes of the fitted
318 curves (Table S1 and S2, Supplementary Material).

319 Porosity of films was also defined (Henriksson & Berglund, 2007). The difference
320 between porosity of cotton- and flax-CNC films could be explained by the higher chance of
321 aggregation for flax-CNC films, which was proven earlier (Csiszár & Nagy, 2017). Thus,
322 cotton-CNC films are denser and less porous than flax-CNC films, containing more
323 aggregated regions. Statistical analysis showed that cellulose source significantly affects the
324 porosity of films ($p < 0.05$). However, the effect of plasticizer type is not significant. An
325 empirically selected exponentially decaying trend line was fitted in the graph of porosity
326 versus the amount of cross-linking agent. Fitted curves for sorbitol and glycerol plasticized
327 cotton- or flax-CNC results are joint, because of the insignificant effect of plasticizer type on
328 film porosity. Analysis of variance showed that there is no significant difference between the
329 shape of the fitted curves (Table S3 and S4 in Supplementary Material). In a previous study,
330 similar results were presented concerning the effect of cellulose source and plasticizer on the
331 porosity of CNC films (Csiszár & Nagy, 2017). When increasing the amount of cross-linking
332 agent, porosity values decrease: from around 16 to 12, and from 25 to 21 % for cotton- and
333 flax-CNC films, respectively (Figs. 3c and d). This is caused by the cross-linking agent that

334 fills the porous parts of CNC films. Minimum porosity is reached at c.a. 20 % cross-linking
335 agent content, in all four groups. Thus, porosity can be adjusted by setting the cross-linker
336 amount. Less porous structure adsorbs less water, which phenomenon was examined
337 henceforward.

338 The crystallinity of cellulose in some compositions of CNC films (prepared with both
339 plasticizers at 0, 10 and 30 % AA content) was also characterized by XRD (Table 1). While in
340 the original cotton and flax ground fibres the crystallinity of cellulose was 75.9 % and 64.8 %,
341 respectively, the crystallinity in CNC films is significantly higher, since the acidic hydrolysis
342 removed the non-crystalline constituents from the fibres. The values range from 83.5 % to
343 93.6 % and depend slightly on both the cellulose source and the type of plasticizers. This
344 means that the crystallinity of flax CNC-films and films plasticized with glycerol is slightly
345 smaller compared to the cotton CNC-films and films plasticized with sorbitol, respectively.
346 Furthermore, the crystallinity slightly decreases with the increasing cross-linking agent
347 content of films. The lower crystallinity can be explained by the smaller lateral dimension of
348 the fibrillar units in nanocrystals, which was created by interfibrillar swelling (Krässig, 1993).
349 Swelling can disrupt the naturally existing aggregations of nanocrystals and increases the
350 accessible surface of particles. The greater the reactive surface is, the smaller the lateral
351 dimensions of the nanocrystals are. Consequently, the smaller lateral dimensions involve an
352 increased interaction with the cross-linking agent and result in a more diffuse equatorial X-ray
353 diffraction. Since flax-CNC has a higher aggregation ability, and glycerol is a better
354 plasticizer than sorbitol (Csiszár & Nagy, 2017), the decrease in crystallinity is more
355 pronounced in the cross-linked flax-CNC films plasticized with glycerol. More significant
356 decrease in crystallinity of polyhydroxybutyrate (PHB) was observed due to the presence of
357 residual amorphous PVA used as an emulsifier in the formation of PHB nanospheres (Abid,
358 Raza, & Rehman, 2016).

359 *3.3 Interaction with water*

360 In the next experiments the interaction of CNC films with liquid water and water
361 vapour was investigated. First, the surface energetics of films was characterized and the
362 dispersion (γ_{SV}^d) and polar (γ_{SV}^p) components of surface free energy were determined by
363 contact angle measurements against water and diiodomethane. All cotton- and flax-CNC neat
364 films display small water contact angles of about 16 °, indicating good wetting property and
365 high hydrophilicity. Water contact angles of the neat cotton and flax films increase
366 significantly from about 16 to 70 °, while the contact angles against diiodomethane decreases
367 only by about 30-40 %, with the increasing amount of cross-linking agent in the range of 0-30
368 % (Table 2). Based on the contact angle data, the surface free energy of CNC films was
369 calculated. Results prove that the total surface free energy values decrease from 74-76 to 53-
370 54 mJ/m² when increasing the amount of cross-linking agent (Table 2). However, the total
371 surface free energy values hardly differ for the films derived from different cellulose sources
372 and cast with different plasticizers. For neat CNC films prepared by spin-coating, the
373 equilibrium water and diiodomethane contact of angles of 23.7 and 27.8 °, respectively, were
374 measured, and a slightly lower surface free energy (58 mJ/m²) was calculated (Aulin et al.,
375 2009).

376 Changes in the dispersion (γ_{SV}^d) and polar (γ_{SV}^p) components of surface free energy as
377 a function of concentration of cross-linking agent are presented in Figs. 4 a and b for cotton-
378 CNC and flax-CNC films, respectively. The shape of the relevant curves appears to be
379 roughly the same for all films, indicating that only the amount of cross-linking agent affects
380 the surface energetic. By increasing the concentration of cross-linking agent, the dispersion
381 component of the surface free energy (γ_{SV}^d) increases slightly (from about 42 to 47 mJ/m²),
382 while the polar component (γ_{SV}^p) decreases drastically (from about 33 to 5 mJ/m²). Since the
383 γ_{SV}^d values of the surface free energy are larger than the γ_{SV}^p ones for both the neat and

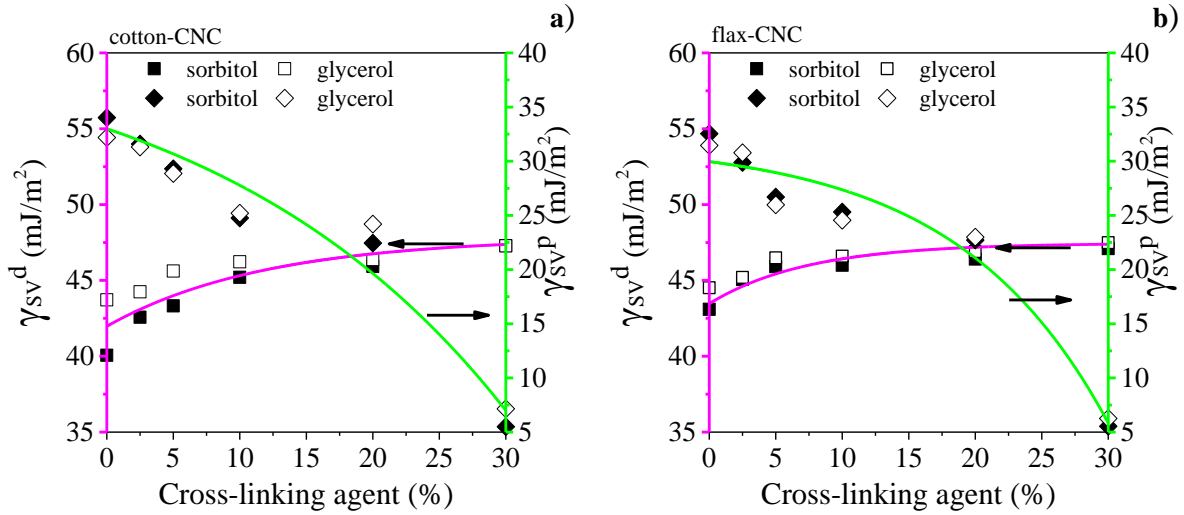
384 composite films, the surface of CNC films is basic in character and has an electron donor
 385 property.

386 **Table 2**

387 Contact angles against water and diiodomethane, and surface free energy of cotton-CNC and
 388 flax-CNC films, plasticized with sorbitol or glycerol and prepared with different amount of
 389 amino-aldehyde based cross-linking agent.

Characte- ristics	Source of cellulose	Type of plasticizer	Concentration of cross-linking agent (%)					
			0	2.5	5	10	20	30
Water contact angle (°)	Cotton	Sorbitol	17 ± 2	20 ± 3	25 ± 3	33 ± 2	37 ± 1	70 ± 4
		Glycerol	16 ± 4	18 ± 1	23 ± 2	31 ± 3	33 ± 3	66 ± 2
	Flax	Sorbitol	16 ± 3	21 ± 4	28 ± 3	31 ± 4	36 ± 5	70 ± 1
		Glycerol	17 ± 2	18 ± 2	29 ± 1	32 ± 3	35 ± 2	68 ± 2
Diiodo- methane contact angle (°)	Cotton	Sorbitol	39 ± 3	34 ± 3	32 ± 2	28 ± 2	26 ± 2	22 ± 1
		Glycerol	31 ± 2	30 ± 3	26 ± 2	25 ± 2	24 ± 2	22 ± 3
	Flax	Sorbitol	33 ± 3	28 ± 1	26 ± 3	25 ± 3	24 ± 3	22 ± 2
		Glycerol	29 ± 2	28 ± 2	24 ± 2	24 ± 3	23 ± 2	21 ± 3
Surface free energy (mJ/m ²)	Cotton	Sorbitol	74	74	73	70	68	53
		Glycerol	76	76	74	71	71	54
	Flax	Sorbitol	76	75	73	71	69	53
		Glycerol	76	76	72	71	70	54

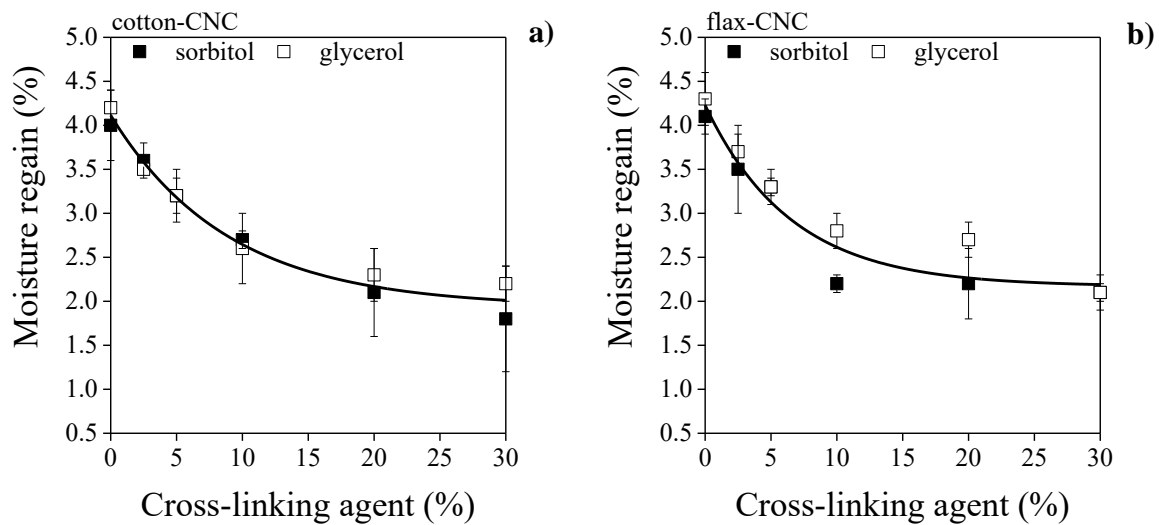
390



391
 392 **Fig. 4.** Dispersion (γ_{sv}^d) and polar components (γ_{sv}^p) of surface free energy of cotton-CNC (a)
 393 and flax-CNC (b) films, plasticized with sorbitol or glycerol, as a function of amino-aldehyde
 394 based cross-linker concentration.

395 Moisture regain is related to the accessible internal surface in the conditioned cotton
 396 fibre (Bertoniere & King, 1992; Krässig, 1993). Moisture regain at 55 % relative humidity
 397 reveals that CNC films with more cross-linking agent absorb less water. Data in Figs. 5a and
 398 b decrease gradually from about 4 to 2 %. The deposition of cross-linking agent on the surface
 399 of cellulose nanocrystals and between the nanocrystals decreases the porosity of films (Figs.
 400 3c and d) and also the available internal cellulose surfaces for water vapour sorption, resulting
 401 in a lower amount of absorbed water (Figs. 5a and b). There is no difference in moisture
 402 regain of cotton-CNC and flax-CNC films, thus the source of cellulose and the type of
 403 plasticizer do not affect the moisture regain values, whereas their dependence on the
 404 concentration of AA cross-linker is obvious. The shape of curves in Figs 5a and b is similar,
 405 indicating that each film with the same cross-linking agent content absorbs water vapour at
 406 approximately the same rate. Due to the cross-linking reaction at higher concentrations, the
 407 amount of accessible hydroxyl groups on the surface of nanocrystals decreases and, as a
 408 result, the interaction of cellulose with water is hindered. Thus, cross-linking suppresses the

409 water sorption of CNC films, and the moisture regain data suggest a decrease in the internal
410 surface in the conditioned CNC films.



411
412 **Fig. 5.** Moisture regain of cotton-CNC (a) and flax-CNC films (b), plasticized with sorbitol or
413 glycerol, as a function of amino-aldehyde based cross-linker concentration.

414 Results of dynamic sinking test (Fig. 6a) reveal that progressive cross-linking causes
415 an increase in sinking time. Immersion of films laid onto the surface of distilled water
416 depends largely on the surface energetic and morphology of films. All changes in these
417 parameters that occurred during cross-linking affect the sinking behaviour of films. Sinking
418 time as a function of the amount of cross-linker shows a general growing trend, which is
419 evident from the data of all four series of films (Fig. 6a). Sinking time data were higher for
420 cotton-CNC films (11-30 min) than for flax-CNC films (4-17 min), which can be attributed to
421 the higher porosity of the flax-CNC films (Fig. 3 d). Sorbitol plasticized films show higher
422 values (6-30 min) than films made with glycerol (4-22 min). The highest sinking time (30
423 min) was measured for the sorbitol plasticized cotton-CNC film with 20 % cross-linking agent
424 content. It has to be mentioned that Fig. 6a does not show the data of films with 30 % cross-
425 linking agent, since they do not immerse at all during the 2-hour dynamic test.

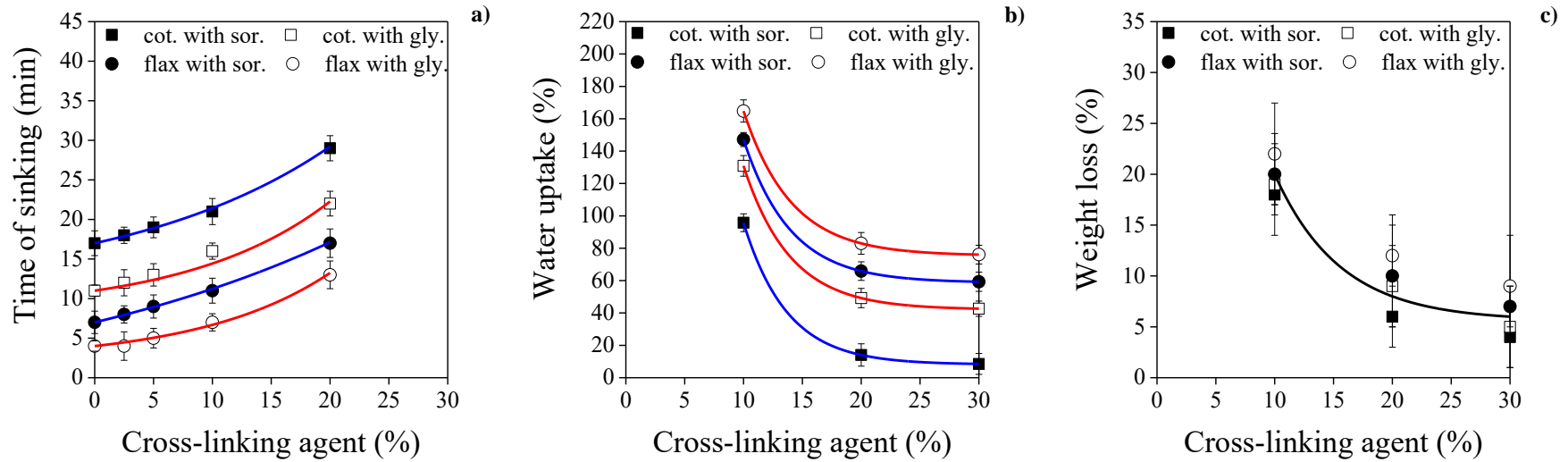
426 Furthermore, it was also observed that the treatment in water under orbital shaking
427 disintegrates the films at lower concentrations of cross-linking agent (0, 2, 5 and 10 %) into
428 cellulose nanocrystals and their aggregates during the course of two hours. However, cross-
429 linking agent with a concentration of 20 % or more prevents delamination and preserves the
430 original shape of films. At higher concentrations of a cross-linker, besides the filling of pores,
431 another process, i.e. cross-linking also occurs (Frick & Harper, 1982) resulting in a water
432 resistant CNC film. For spin-coated films, a heat-treatment at 90 °C for 4 hours was applied to
433 avoid delamination upon exposure to an aqueous solution (Aulin et al., 2009).

434 To investigate further the interaction of films with water, we developed a method to
435 measure the water uptake of films. For textiles and fibres, the method of water of imbibition
436 provides similar (but not identical) information on water holding capacity and reflects the
437 internal volume of the fibres in the water-swollen state (Bertoniere, Martin, Florine, &
438 Rowland, 1972). For films, the values of water uptake derived from the static sinking test can
439 be related to the internal volume of cellulose in the swollen state and can also be used for
440 characterizing the rate of swelling. From the results of water uptake plotted in Fig. 6b it
441 appears that maximum swelling occurs at 10 % cross-linking agent concentration, the values
442 are higher for the flax-CNC films (160 and 130 %) than for the cotton-CNC ones (150 and
443 100 %) and also higher for the glycerol plasticized films than for the sorbitol plasticized ones
444 (160 and 150 % vs. 130 and 100 %, respectively). Results also reveal that with increasing the
445 concentration of cross-linking agent from 10 to 20 % the water uptake decreases abruptly.
446 Then the water uptake levels off at about 20 % cross-linking agent content. This correlates
447 well with the tendencies of film porosity in Figs. 3c and d, since both porosity and water
448 uptake decrease with increasing cross-linking agent content and the minimum values in both
449 are reached at 20 % cross-linking agent content. In addition, the films with 20 and 30 % cross-

450 linker content display similar swelling behaviour, their water uptake is under 10 %, indicating
451 a compact and tightly bound structure.

452 It is also obvious that when the time of sinking or the water uptake are plotted against
453 cross-linking agent concentration in Figs 6a and b, respectively, the differences between the
454 films tested become much more apparent than in the relationships obtained in the preceding
455 experiments. It means that the extent of properties mentioned here depends not only on the
456 concentration of cross-linking agent, but also on the source of cellulose and the type of
457 plasticizers.

458 It was observed that films with lower cross-linking agent content (0, 2.5 and 5 %) have
459 'disappeared' during the course of treatment, which may result from the delamination of
460 nanocrystals by a progressive and infinite swelling of films. However, films with a cross-
461 linking agent concentration of 10 % or more retain their shape and besides the water uptake,
462 the dried weight can also be determined. The results in Fig. 6c reveal the weight loss of films
463 at equal cross-linking agent content that occurred over the course of 24 hours is very similar,
464 indicating that neither the source of cellulose nor the type of plasticizer affects the data. Thus,
465 the extent of weight loss depends only on the concentration of cross linking agent. The most
466 water resistant films contain 30 % of cross-linking agent and their weight decreases only by
467 about 5 %. At 10 % of cross-linking agent, however, about the 20 weight % of films is
468 released, which may be attributed to the removal of plasticizer and/or the disruption of the
469 edges of films. Information from swelling experiments gives further evidence about the wet-
470 curing of nanocrystals with an amino-aldehyde based compound.



471

472 **Fig. 6.** Results of sinking tests of cotton-CNC and flax-CNC films plasticized with sorbitol or glycerol, as a function of the amount of amino-
 473 aldehyde based cross-linking agent. Dynamic sinking test: (a) sinking time as a function of cross-linking agent content (0, 2.5, 5, 10 and 20 %).
 474 Static sinking test at 10, 20 and 30 % cross-linking agent content: (b) water uptake as a percentage of dry weight of CNC film by swelling over
 475 the course of 24-hours; (c) weight loss of CNC films caused by sinking test over the course of 24-hours. Calculation of values (%) in Figs. b and c
 476 was based on the initial dry weight of films.

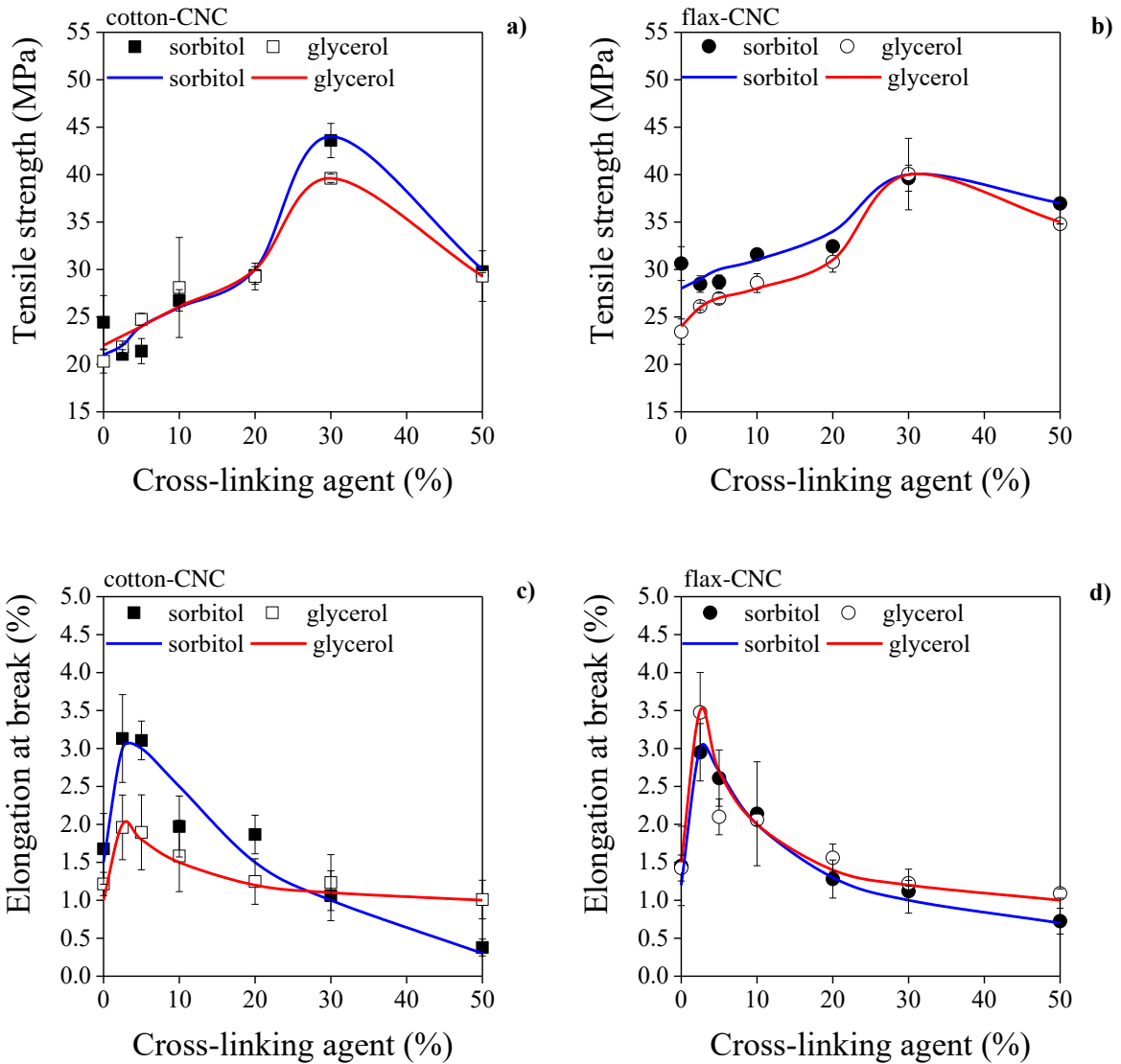
477 *3.4 Mechanical properties of the CNC nanocomposite films*

478 Tensile properties of CNC films were also tested but in a slightly wider concentration
479 range of the cross-linker (0-50 %). Results in Figs 7a and b reveal that the tensile strength of
480 neat films (0 %) increases from about 18-32 MPa to around 40 MPa and then decreases with
481 increasing cross-linking agent concentration. The maximum tensile strength values can be
482 reached at 30 % cross-linker content for all the films tested. The elongation-at-break values
483 also show a maximum (2.5-4 %) at a cross-linking agent concentration of 2.5 % and then
484 decrease sharply. It can be assumed that a small amount of cross-linking agent works also as a
485 plasticizer for nanocellulose (Henriksson & Berglund, 2007). Results in the former chapters
486 proved that a concentration of 2.5-5 % is not enough for building a cross-linked structure
487 between the cellulose nanocrystals. Nevertheless, by penetrating into the connection points
488 between the nanocrystals during the course of a simultaneous casting-wet curing and covalent
489 bonding to the accessible hydroxyl groups of cellulose surfaces, the cross-linking agent can
490 prevent the development of a hydrogen bonding network in CNC films. Since this hydrogen
491 bonded structure is responsible for the stiffness of films, cross-linking agent at low
492 concentrations contributes to slipping of nanocrystals on each other. However, at higher
493 concentrations the stiffness of films is higher and the elongation-at-break values decrease to
494 0.3-1.2 %. This proves that at higher cross-linking agent concentration (> 5 %) cellulose
495 nanocrystals are cross-linked in CNC films.

496 The modulus of films was determined from the initial slope of typical stress-strain
497 curves (Table 3). It was found that modulus increases (from 3-6 GPa to 9-11 GPa) with the
498 increasing amount of cross-linking agent in films. The maximum modulus value achieved was
499 higher for cotton-CNC (c.a. 11 GPa) then for flax-CNC (c.a. 9 GPa). The type of plasticizer
500 does not especially affect the values, however, at lower cross-linking agent concentrations,
501 some diversity with respect to modulus can be observed.

502 Furthermore, the moduli in Table 3 show correlations with the crystallinity indices in
 503 Table 1 since films with higher extent of crystallinity tend to have higher modulus. The
 504 correlation coefficients were found to be 0.5943, 0.3527 and 0.6489 for the films prepared
 505 with 0, 10 and 30 % cross-linking agent, respectively.

506



507

508

509 **Fig. 7.** Tensile strength (a, b) and elongation at break (c, d) of CNC films from cotton (a, c)
 510 and flax (b, d), plasticized with sorbitol or glycerol, made with different amount of cross-
 511 linker. The uncertainty of data is represented by a 95 % confidence interval.

512

513 **Table 3**

514 Young's modulus (GPa) of cotton-CNC and flax-CNC films plasticized with sorbitol or
 515 glycerol and prepared with different amount of amino-aldehyde based cross-linking agent.

Concentration of cross-linking agent (%)	Source of cellulose			
	Cotton		Flax	
	Type of plasticizer			
	Sorbitol	Glycerol	Sorbitol	Glycerol
0	5.56 ± 0.53	4.19 ± 0.61	5.01 ± 0.45	3.21 ± 0.32
2.5	2.76 ± 0.74	2.23 ± 0.71	3.12 ± 0.39	2.12 ± 0.81
5	3.53 ± 0.55	2.61 ± 0.58	4.03 ± 0.58	2.53 ± 0.74
10	4.89 ± 0.81	4.07 ± 0.72	5.47 ± 0.61	3.51 ± 0.81
20	8.37 ± 0.32	5.61 ± 0.39	6.41 ± 0.76	5.27 ± 0.32
30	9.91 ± 0.81	6.83 ± 0.76	8.72 ± 0.72	7.39 ± 0.55
50	11.22 ± 0.32	10.57 ± 0.45	9.03 ± 0.71	8.52 ± 0.53

516

517 The effect of cross-linking of nanocellulose with different reagents was also reported
 518 in the scientific literature. When nanopaper was cross-linked by first soaking it in 16 wt %
 519 citric acid solution in the presence of 1 wt % sodium hypophosphate (pH 2) overnight and
 520 then curing at 160 °C for 10 min in a hot-press, its mechanical properties were not improved
 521 in dry state, but the modulus was increased from 5.3 to 8.5 GPa. Furthermore, the wet
 522 strength of the cross-linked nanopaper improved significantly and an almost ten-fold increase
 523 in the stress to failure value was detected (Quellmalz & Mihranyan, 2015).

524 4. Discussion

525 Transparent and smooth nanocomposite films were prepared from cellulose
526 nanocrystals extracted from cotton and flax fibres, with different plasticizers (sorbitol,
527 glycerol) and an amino-aldehyde based cross-linking agent in a wide composition range (0-30
528 wt %), during the course of a simultaneous casting and wet curing. The effect of cross-linker
529 concentration on the morphology, optical and tensile properties of films was investigated, and
530 the interaction of films with liquid water and water vapour was also characterized by various
531 measurements. Results showed that properties of films were substantially affected by the
532 concentration of cross-linking agent, but were only slightly influenced by the source of
533 cellulose and type of plasticizers.

534 While the transparency of films was unaffected, the haze-index decreased significantly
535 with the increasing concentration of cross-linker. SEM micrographs revealed that the
536 fractured surface of the cross-linked films became slightly rougher comparing to the neat
537 counterparts. Density increased and porosity decreased when cross-linking occurred, and a
538 maximum density and a minimum porosity were reached at an amino-aldehyde concentration
539 of 20 %. Furthermore, the crystallinity of cellulose in the composite films slightly decreased
540 with the increasing concentration of cross-linking agent. Besides the cross-linking agent
541 content, the source of cellulose and the type of plasticizer had also an effect on the
542 crystallinity.

543 All cotton- and flax-CNC neat films displayed small water contact angles of about 16
544 °, indicating good wetting property and high hydrophilicity. Significantly higher water contact
545 angles were measured for the cross linked films (66-70 ° at 30 % cross-linker concentration)
546 and simultaneously a drastic decrease (from about 33 to 5 mJ/m²) in the polar component
547 (γ_{SV}^p) of surface free energy was calculated. The surface of CNC films is basic in character
548 and has an electron donor property. Cross-linked films with a less porous structure absorbed

549 less water. Moisture regain decreased with the increasing amount of the cross-linking agent,
550 indicating a decrease in the internal surface in the conditioned CNC films. Furthermore,
551 cross-linking suppressed the swelling determined by water uptake, and prevented the
552 delamination of CNC films at a cross-linker concentration of 10 % or higher.

553 The tensile strength of CNC films first increased from about 18-32 MPa to around 40
554 MPa and then decreased with increasing cross-linking agent concentration. The maximum
555 tensile strength was measured at 30 % cross-linker content. Elongation-at-break values also
556 reached a maximum (2.5-4 %) at a cross-linking agent concentration of 2.5 %, suggesting that
557 the small amount of cross-linking agent worked as a plasticizer for nanocellulose. All the
558 presented results demonstrated that the structure and properties of CNC films can be modified
559 and tuned by cross-linking with and amino-aldehyde based compound.

560 5. Conclusions

561 In the frame of this study, cellulose nanocrystal/amino-aldehyde biocomposite films
562 were prepared and characterized. In the simultaneous casting and wet cross-linking process
563 the nanocellulose particles had enough time for self-ordering and forming a compact three-
564 dimensional layered structure. The cross-linking agent made the interactions of CNC particles
565 stronger and modified the optical and tensile properties as well as the morphology of films.
566 Furthermore, a significant improvement in water resistance was achieved. The effect of the
567 cross-linking agent in the applied concentration range was more significant than that of the
568 cellulose source (cotton or flax) or the type of plasticizers (sorbitol or glycerol).

569 6. References

570 Abid, S., Raza, Z. A., & Rehman, A. (2016). Synthesis of poly(3-hydroxybutyrate) nanospheres
571 and deposition thereof into porous thin film. *Materials Research Express*, 3(10).
572 <https://doi.org/10.1088/2053-1591/3/10/105042>

573 Abraham, E., Kam, D., Nevo, Y., Slattegard, R., Rivkin, A., Lapidot, S., & Shoseyov, O.
574 (2016). Highly Modified Cellulose Nanocrystals and Formation of Epoxy-Nanocrystalline
575 Cellulose (CNC) Nanocomposites. *ACS Applied Materials and Interfaces*, 8(41), 28086–
576 28095. <https://doi.org/10.1021/acsami.6b09852>

577 Aulin, C., Ahok, S., Josefsson, P., Nishino, T., Hirose, Y., Österberg, M., & Wågberg, L.
578 (2009). Nanoscale cellulose films with different crystallinities and mesostructures - Their
579 surface properties and interaction with water. *Langmuir*, 25(13), 7675–7685.
580 <https://doi.org/10.1021/la900323n>

581 Belbekhouche, S., Bras, J., Siqueira, G., Chappey, C., Lebrun, L., Khelifi, B., ... Dufresne, A.
582 (2011). Water sorption behavior and gas barrier properties of cellulose whiskers and
583 microfibrils films. *Carbohydrate Polymers*, 83(4), 1740–1748.
584 <https://doi.org/10.1016/j.carbpol.2010.10.036>

585 Bertoniere, N. R., & King, W. D. (1992). Pore Structure of Cotton Fabrics Crosslinked with
586 Formaldehyde-Free Reagents. *Textile Research Journal*, 62(6), 349–356.
587 <https://doi.org/10.1177/004051759206200607>

588 Bertoniere, N. R., Martin, L. F., Florine, A. B., & Rowland, S. P. (1972). Alteration of the pore
589 structure of cotton by the wet-fixation durable-press process. *Textile Research Journal*,
590 42(12), 734–740.

591 Csiszar, E., Kalic, P., Kobol, A., & Ferreira, E. D. P. (2016). The effect of low frequency
592 ultrasound on the production and properties of nanocrystalline cellulose suspensions and
593 films. *Ultrasonics Sonochemistry*, 31, 473–480.
594 <https://doi.org/10.1016/j.ultsonch.2016.01.028>

595 Csiszár, E., & Nagy, S. (2017). A comparative study on cellulose nanocrystals extracted from
596 bleached cotton and flax and used for casting films with glycerol and sorbitol plasticisers.

597 *Carbohydrate Polymers*, 174, 740–749. <https://doi.org/10.1016/j.carbpol.2017.06.103>

598 Devallencourt, C., Saiter, J. M., & Capitaine, D. (2000). Reactions between melamine
599 formaldehyde resin and cellulose: Influence of pH. *Journal of Applied Polymer Science*,
600 78(11), 1884–1896. [https://doi.org/10.1002/1097-4628\(20001209\)78:11<1884::AID-APP60>3.0.CO;2-2](https://doi.org/10.1002/1097-4628(20001209)78:11<1884::AID-APP60>3.0.CO;2-2)

601

602 Frick, J. G., & Harper, R. J. (1982). Crosslinking cotton cellulose with aldehydes. *Journal of*
603 *Applied Polymer Science*. <https://doi.org/10.1002/app.1982.070270317>

604 Hamad, W. Y., & Hu, T. Q. (2010). Structure-process-yield interrelations in nanocrystalline
605 cellulose extraction. *Canadian Journal of Chemical Engineering*, 88(3), 392–402.
606 <https://doi.org/10.1002/cjce.20298>

607 He, W., Goudeau, P., Le Bourhis, E., Renault, P. O., Dupré, J. C., Doumalin, P., & Wang, S.
608 (2016). Study on Young's modulus of thin films on Kapton by microtensile testing
609 combined with dual DIC system. *Surface and Coatings Technology*, 308, 273–279.
610 <https://doi.org/10.1016/j.surfcoat.2016.07.114>

611 Henriksson, M., & Berglund, L. A. (2007). Structure and properties of cellulose nanocomposite
612 films containing melamine formaldehyde. *Journal of Applied Polymer Science*, 106(4).
613 <https://doi.org/10.1002/app.26946>

614 Kim, E., & Csiszár, E. (2005). Chemical Finishing of Linen and Ramie Fabrics. *Journal of*
615 *Natural Fibers*, (2:3), 39–52. <https://doi.org/10.1300/J395v02n03>

616 Klemm, D., Kramer, F., Moritz, S., Lindström, T., Ankerfors, M., Gray, D., & Dorris, A.
617 (2011). Nanocelluloses: A new family of nature-based materials. *Angewandte Chemie -*
618 *International Edition*, 50(24), 5438–5466. <https://doi.org/10.1002/anie.201001273>

619 Krässig, H. A. (1993). *Cellulose: Structure, accessibility and reactivity*. Gordon and Breach

620 Science Publishers, Switzerland.

621 Lagerwall, J. P. F., Schütz, C., Salajkova, M., Noh, J., Hyun Park, J., Scalia, G., & Bergström,
622 L. (2014). Cellulose nanocrystal-based materials: from liquid crystal self-assembly and
623 glass formation to multifunctional thin films. *NPG Asia Materials*, 6(1), 1–12.
624 <https://doi.org/10.1038/am.2013.69>

625 Larsson, P. T., Hult, E., Wickholm, K., Pettersson, E., & Iversen, T. (1999). CPrMAS 13 C-
626 NMR spectroscopy applied to structure and interaction studies on cellulose I. *Solid State*
627 *Nuclear Magnetic Resonance*, 15, 31–40. [https://doi.org/10.1016/S0926-2040\(99\)00044-](https://doi.org/10.1016/S0926-2040(99)00044-2)
628 2

629 Liu, Y., Li, Y., Yang, G., Zheng, X., & Zhou, S. (2015). Multi-stimulus-responsive shape-
630 memory polymer nanocomposite network cross-linked by cellulose nanocrystals. *ACS*
631 *Applied Materials and Interfaces*, 7(7), 4118–4126. <https://doi.org/10.1021/am5081056>

632 Majoinen, J., Kontturi, E., Ikkala, O., & Gray, D. G. (2012). SEM imaging of chiral nematic
633 films cast from cellulose nanocrystal suspensions. *Cellulose*, 19(5), 1599–1605.
634 <https://doi.org/10.1007/s10570-012-9733-1>

635 Mathew, A. P., & Dufresne, A. (2002). Plasticized waxy maize starch: Effect of polyols and
636 relative humidity on material properties. *Biomacromolecules*, 3(5), 1101–1108.
637 <https://doi.org/10.1021/bm020065p>

638 Niinivaara, E., Faustini, M., Tammelin, T., & Kontturi, E. (2015). Water vapor uptake of
639 ultrathin films of biologically derived nanocrystals: Quantitative assessment with quartz
640 crystal microbalance and spectroscopic ellipsometry. *Langmuir*, 31(44), 12170–12176.
641 <https://doi.org/10.1021/acs.langmuir.5b01763>

642 Owens, D. K., & Wendt, R. C. (1969). Estimation of the surface free energy of polymers.

643 *Journal of Applied Polymer Science*, 13(8), 1741–1747.
644 <https://doi.org/10.1002/app.1969.070130815>

645 Pakzad, A., Simonsen, J., & Yassar, R. S. (2012). Gradient of nanomechanical properties in the
646 interphase of cellulose nanocrystal composites. *Composites Science and Technology*,
647 72(2), 314–319. <https://doi.org/10.1016/j.compscitech.2011.11.020>

648 Peng, P., Zhai, M., She, D., & Gao, Y. (2015). Synthesis and characterization of carboxymethyl
649 xylan-g-poly(propylene oxide) and its application in films. *Carbohydrate Polymers*, 133,
650 117–125. <https://doi.org/10.1016/j.carbpol.2015.07.009>

651 Quellmalz, A., & Mihranyan, A. (2015). Citric Acid Cross-Linked Nanocellulose-Based Paper
652 for Size-Exclusion Nanofiltration. *ACS Biomaterials Science and Engineering*, 1(4), 271–
653 276. <https://doi.org/10.1021/ab500161x>

654 Raza, Z. A., Riaz, S., & Banat, I. M. (2017). Polyhydroxyalkanoates: Properties and chemical
655 modification approaches for their functionalization. *Biotechnology Progress*.
656 <https://doi.org/10.1002/btpr.2565>

657 Rouette, H. K. (2002). *Encyclopedia of textile finishing*. Springer, Berlin, Heidelberg.

658 Roy Choudhury, A. K. (2014). *Principles of Colour and Appearance Measurement. Principles*
659 *of Colour and Appearance Measurement* (Vol. 2). [https://doi.org/10.1016/C2014-0-](https://doi.org/10.1016/C2014-0-01832-1)
660 01832-1

661 Segal, L., Creely, J. J., Martin, A. E., & Conrad, C. M. (1959). An Empirical Method for
662 Estimating the Degree of Crystallinity of Native Cellulose Using the X-Ray
663 Diffractometer. *Textile Research Journal*, 29(10), 786–794.
664 <https://doi.org/10.1177/004051755902901003>

665 Si, J., Cui, Z., Wang, Q., Liu, Q., & Liu, C. (2016). Biomimetic composite scaffolds based on

666 mineralization of hydroxyapatite on electrospun poly(ϵ -caprolactone)/nanocellulose
667 fibers. *Carbohydrate Polymers*, 143, 270–278.
668 <https://doi.org/10.1016/j.carbpol.2016.02.015>

669 Sun, Q., Zhao, X., Wang, D., Dong, J., She, D., & Peng, P. (2018). Preparation and
670 characterization of nanocrystalline cellulose/*Eucommia ulmoides* gum nanocomposite
671 film. *Carbohydrate Polymers*, 181, 825–832.
672 <https://doi.org/10.1016/j.carbpol.2017.11.070>

673 Tang, J., Sisler, J., Grishkewich, N., & Tam, K. C. (2017). Functionalization of cellulose
674 nanocrystals for advanced applications. *Journal of Colloid and Interface Science*, 494,
675 397–409. <https://doi.org/10.1016/j.jcis.2017.01.077>

676 Wang, L. E. I., Kamal, M. R., & Rey, A. D. (2001). Light Transmission and Haze of
677 polyethylene blown thin films. *Polymer Engineering & Science*, 41(2), 358–372.

678 Yang, J., Zhao, J. J., Xu, F., & Sun, R. C. (2013). Revealing strong nanocomposite hydrogels
679 reinforced by cellulose nanocrystals: Insight into morphologies and interactions. *ACS*
680 *Applied Materials and Interfaces*, 5(24), 12960–12967.
681 <https://doi.org/10.1021/am403669n>

682

683

684